IEEE/CSC & ESAS EUROPEAN SUPERCONDUCTIVITY NEWS FORUM (ESNF), No. 10, October 2009.
Published in *AIP Conference Proceedings* **1219**, pp. 362-369 (2010)

SECOND PHASE ($BaGeO_3$, $BaSiO_3$) NANOCOLUMNS IN $YBa_2Cu_3O_{7-x}$ FILMS

C. V. Varanasi[1,4], J. Reichart[4], J. Burke[1,4],
H. Wang[2], M. Susner[3], M. Sumption[3], P.N. Barnes[4]

[1] University of Dayton Research Institute Dayton
Dayton, OH, 45469-0170, USA

[2] Texas A&M
College Station, TX, 77843-3128, USA

[3] The Ohio State University
Columbus, OH, 43210, USA

[4]Air Force Research Laboratory
Wright-Patterson AFB, OH, 45433, USA

ABSTRACT

$YBa_2Cu_3O_{7-x}$ (YBCO) films with $BaGeO_3$ (BGeO), $BaSiO_3$ (BSiO) second phase additions were processed by pulsed laser deposition. Sectored targets with BGO or BSiO wedges as well as pre-mixed targets of YBCO, BGeO or BSiO with appropriate compositions were used to deposit YBCO+BGeO and YBCO+BSiO films on (100) single crystal $LaAlO_3$ substrates. The cross-sectional transmission electron micrographs showed the presence of 20 nm diameter nanocolumns in the YBCO films of both the compositions. However, the critical transition temperature (T_c) of the films was found to significantly decrease. As a result, the critical current density (J_c) in applied magnetic fields was suppressed. The YBCO+BGeO and YBCO+BSiO films made with lower concentrations of additions showed slight improvement in T_c indicating that the substitution of Ge and Si in the lattice is possibly responsible for the T_c depression. This study shows that in addition to the ability to form nanocolumns, the chemical compatibility of $BaSnO_3$ (BSO) and $BaZrO_3$ (BZO) as observed in YBCO+BSO and YBCO+BZO is critical to process high J_c YBCO films

KEYWORDS: Flux pinning, $BaSnO_3$, $BaGeO_3$, $BaSiO_3$, $YBa_2Cu_3O_{7-x}$, coated conductors, pulsed laser deposition

INTRODUCTION

$YBa_2Cu_3O_{7-x}$ (YBCO) coated conductors need the introduction of additional flux pinning centers to enhance the critical current density (J_c) in applied magnetic fields [1, 2]. Second phase additions such as $BaZrO_3$ (BZO) [3,4] and $BaSnO_3$ (BSO) [5,6] have shown to form nanocolumnar pinning sites in YBCO films and contribute towards enhancing the critical current density (J_c), especially in the H//c orientation. Up to 20 mol% of BSO additions seem to have no deleterious effects on the critical transition temperature (T_c) [7] of the YBCO+BSO films but enhance J_c by several orders of magnitude at high fields. Typically BSO nanocolumns found to enhance J_c by more than two orders of magnitude at 77 K in applied fields of > 5T in H//C. Even in thick films > 1 μm, the BSO nanocolumns continue to grow perpendicular to ab planes and offer maintenance of high J_c in the films [8]. In the YBCO+BZO system, similar improvements were also noted but it was found that just 5 vol% BZO could reduce the T_c significantly [9].

It appears that for nanocolumnar formation in YBCO, values such as T_c, J_c etc. depends mainly upon the composition of the added second phases as well as the self-assembly of the second phase material into the nanocolumns. Similarly processed YBCO+Y_2BaCuO_5 (Y211) films do not form the nanocolumns. Further, the T_c is not significantly reduced in YBCO+Y211 films but the T_c is slightly reduced in YBCO+BSO films. The T_c reduction indicates a potential chemical compatibility issue for the second phase addition. It is important that the number density of nanocolumns and associated defects need to be increased as high as possible at higher magnetic fields to maximize J_c in YBCO films, without sacrificing the T_c of the films. The number density of nanocolumns also depends upon the composition and concentration of the second phase doping. It is of interest to study what effect different compositions of second phase additions will have on the formation of nanocolumns and superconducting properties (T_c, J_c) of YBCO films. In this study, second phase additions of $BaGeO_3$ (BGeO) and $BaSiO_3$ (BSiO) were investigated for their ability to form nanocolumns and their effect on the T_c and J_c of YBCO films. The intent was to determine the effect of substituting different column IV elements of the periodic table in place of Sn for BSO. The properties were compared with YBCO+BSO films.

EXPERIMENTAL

$BaGeO_3$

BGeO (PDF# 30-0127) has an hexagonal crystal structure with cell dimensions as 7.59 A^o x 7.59 A^o x 10.79 A^o and a density of 4.73g/cm^3. It also has a high temperature orthorhombic form [11,12]. The BGeO target was prepared in-house by solid state reaction from precursor powders of $BaCO_3$ (99.997% purity, Alfa Aesar) and GeO_2 (99.999% purity, Alfa Aesar). The precursor powders were dried at 450°C for 8 hours in alumina crucible. The powders were measured with a 1:1 molar ratio and mixed in an agate mortar for 30 minutes to ensure a homogeneous mixture. The mixed powder was reacted at 1050°C for 48 hours in air. The powder was again mixed using agate mortar and pestle and then was pressed in a hydraulic hand press using a 1.25"dia. die then placed in a furnace and heated to 1050°C for 48 hours. A third heating cycle was run at 1100°C for 48 hours yielding a theoretical density of 57.7%. An additional higher temperature reaction at 1200°C improved the density but showed some evidence of incipient melting. X-ray diffraction patterns were obtained from the ground powder from these disks. Sector pieces

cut from these disks were fixed on top of a YBCO target and was used to make YBCO+ BGeO films.

$BaSiO_3$

BSiO (PDF# 26-1402) has an orthorhombic crystal structure with cell dimensions of 5.6182 A^o x 12.445 A^o x 4.5816 A^o and a density of 4.425 g/cm^3. Ba_2SiO_4 (PDF# 26-1403) is also orthorhombic with a cell size of 7.508 A^o x 10.214 A^o x 5.8091 A^o and a density of 5.468 g/cm^3. $BaSiO_3$ targets were made using $BaSiO_3$ powder purchased from Alfa Aesar. The commercially available powder has a composition corresponding to 74.3% BaO and 21.8% SiO_2. Initially the purchased powder was dried in an alumina crucible at 450°C for 8 hours. The powder was then mixed in agate mortar and then pressed in a hydraulic hand press using a 1.25" dia die. The target was then reacted at 1000°C for 50 hours yielding a density of approximately 64.2% theoretical density. The target was then heated again to 1200°C yielding a density of approximately 90.7% theoretical density. A small section of target was then cut using a diamond saw and ground using agate mortar and pestle and was analyzed using a Rigaku Dmax 2500 X-ray powder diffractometer. Sectors of the BSiO disk were cut and fixed on top of a YBCO target and was used to make YBCO+ BSiO films.

Targets and Deposition

To create the premixed targets of YBCO+BGeO, for example, a 20 gram batch of BGeO was first made by solid sate reaction from precursor powders as discussed above. The precursor powders were dried at 450°C for 8 hours in an alumina crucible. The powders were measured with a 1:1 molar ratio and mixed in an agate mortar with pestle for 30 minutes to ensure a homogeneous mixture. The mixed powder was reacted at 1050°C for 48 hours. The powder was again mixed using agate mortar and pestle and heated to 1050°C for 72 hours. The mix targets were made from Nexans YBCO powder and the BGeO powder previously made. YBCO was dried in an alumina crucible at 450°C for 8 hours. After drying, the powders were mixed using 2 vol% and 4 vol% BGeO to YBCO powder. Each target was thoroughly mixed using agate mortar and pestle and pressed in 1.25" dia. die using a hydraulic press. The targets were then reacted in air at 850°C for 72 hours and 920°C for 168 hours. The targets obtained a density of 93.1% (2 vol.% BGeO) and 91.05% (4 vol.% BGeO) of theoretical density.

All the YBCO+ second phase films were deposited in a Neocera pulsed laser ablation chamber using λ= 248 nm Lambda PhysiK excimer laser. Standard method as used before for processing YBCO+BSO films (780 ^oC growth temperature, 300 m torr O_2 pressure, 625 mJ laser energy, 4 HZ repetition rate) were used to process YBCO+BGeO and YBCO+BSiO films [10]. $LaAlO_3$ (100) single crystal substrates were used to deposit YBCO film with different second phase additions. Sectored targets with 30^o sector of BGeO or a BSiO fixed on top of a YBCO target and premixed targets of 2, 4 vol.% BGeO were used to deposit ~ 300 nm thick films.

Films were characterized by x-ray diffraction and the microstructures were studied by plan view scanning electron microscopy (SEM) and a cross-sectional transmission electron microscopy (TEM). The superconducting properties such as critical transition temperature (Tc) was measured by using a dc susceptibility method in a Physical Property Measurement System (Quantum Design PPMS) and the self field critical current density (J_c) was measured by using a four point probe method on a patterned bridge at 77 K.

RESULTS AND DISCUSSION

FIGURE 1 shows the theta-two theta x-ray diffraction pattern of BGeO powder used for premix targets and sintered BGeO used for sector target. All the peaks corresponding to BGeO were observed indicating that the reaction was mostly complete and the precursors are converted in to $BaGeO_3$. However some small intensity peaks corresponding to some other unidentified phases were also observed to be present in the patterns. Repeated grinding and high temperature reactions did not reduce this unknown phase. In the literature [11, 12] the possibility of formation of other polymorphic phases as well as other phases such as Ba_2GeO_4 were noted in $BaO\text{-}GeO_2$ system. Although the peaks did not match any of the known phases, it is thought that the unknown peaks correspond to some other intermediate phases. FIGURE 2 shows the x-ray powder diffraction patterns taken from $BaSiO_3$ powders used in this study. It can be seen that the commercially available powders contain mixtures of $BaSiO_3$, $BaSi2O_4$. Since both are orthorhombic structures and contain Ba, Si, and O, targets were made using these powders to investigate the nanocolumn formation. In either case, during the PLD, the bonds of these phases are broken and recombine in the growing film to form again.

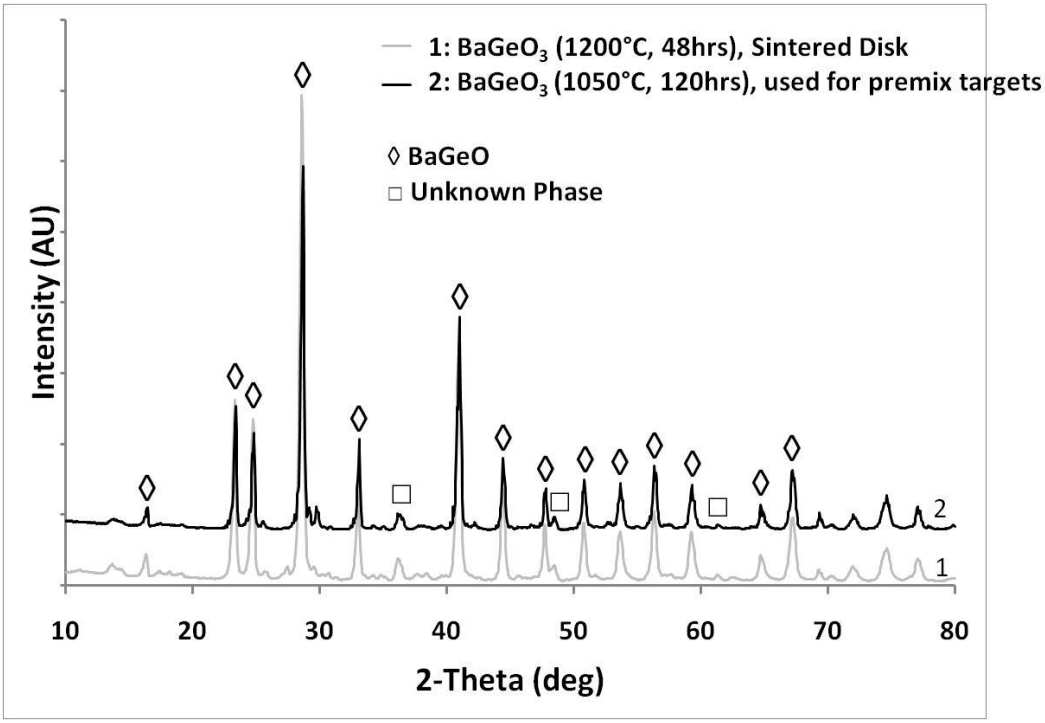

FIGURE 1. X-ray theta-two theta scans of $BaGeO_3$ prepared in the present study

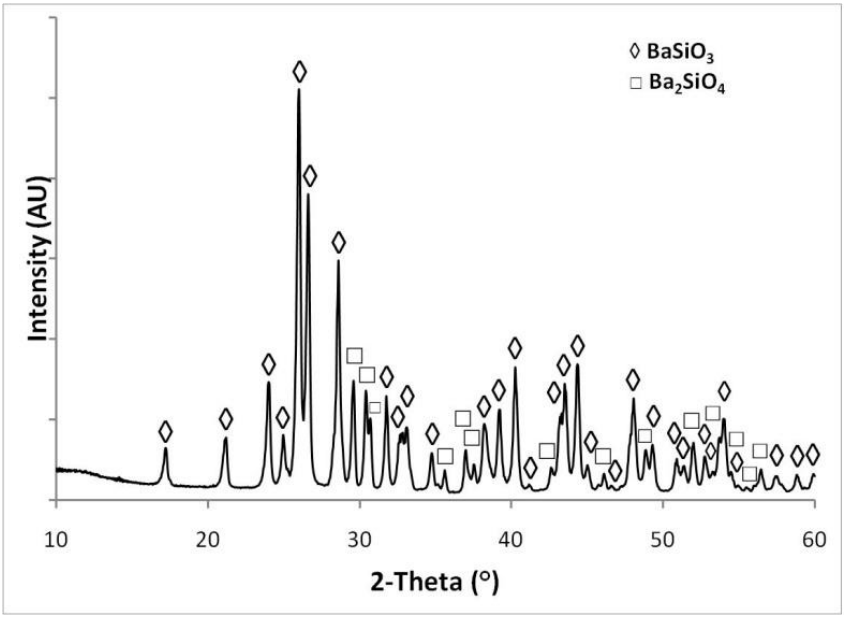

FIGURE 2. X-ray theta- two theta patterns of Ba-Si-O powder used in the present study

FIGURE 3 shows a plan view SEM micrograph of images of YBCO+BGeO and YBCO+BSiO films made by using a sectored target. Good distribution of bright phase (white contrast) that represents the second phase material is found to be well dispersed in the microstructure. Around 20 nm diameter nanoparticles were observed in both the samples. Although they appear as nanoparticles in plan view SEM, these are evidently the cross-sections of nanocolumns as discussed later. The microstructures of YBCO+BGeO and YBCO+BSiO look very similar to YBCO+BSO samples processed in the same fashion.

FIGURE 4 shows cross-sectional transmission electron micrographs of YBCO+BGeO samples in two different magnifications. It can be seen that the nanocolumns are around 20 nm and extend throughout the thickness of the films. As reported earlier, nanocolumns in YBCO+BSO are of 8-10 nm and were found to be very straight. However with YBCO+BGeO, the nanocolumns seem to be almost double in the size and also they were found to be not as straight as BSO. The lattice mismatch and strain between the matrix of YBCO and second phase additions can dictate the equilibrium diameter and splay of the nanocolumns.

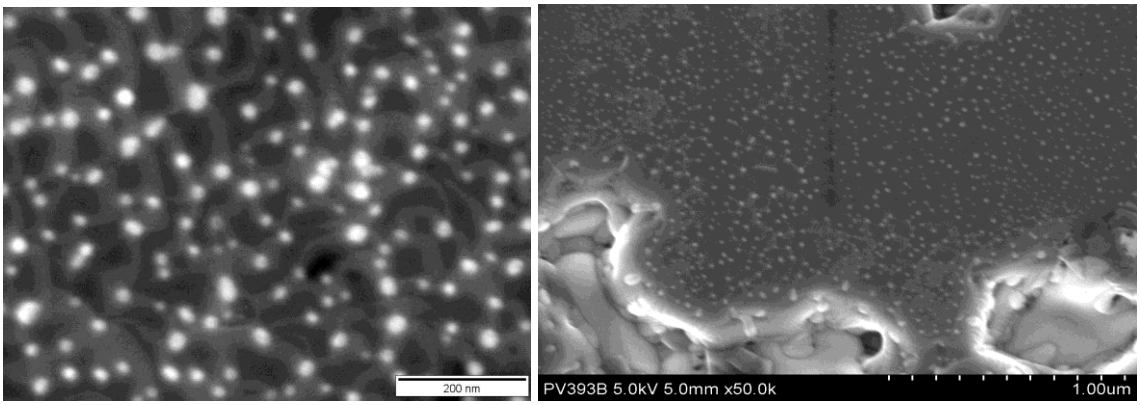

(a) (b)

FIGURE 3. Plan View SEM micrographs of YBCO films made by using a PLD sectored target
a) YBCO+BGeO b) YBCO+BSiO

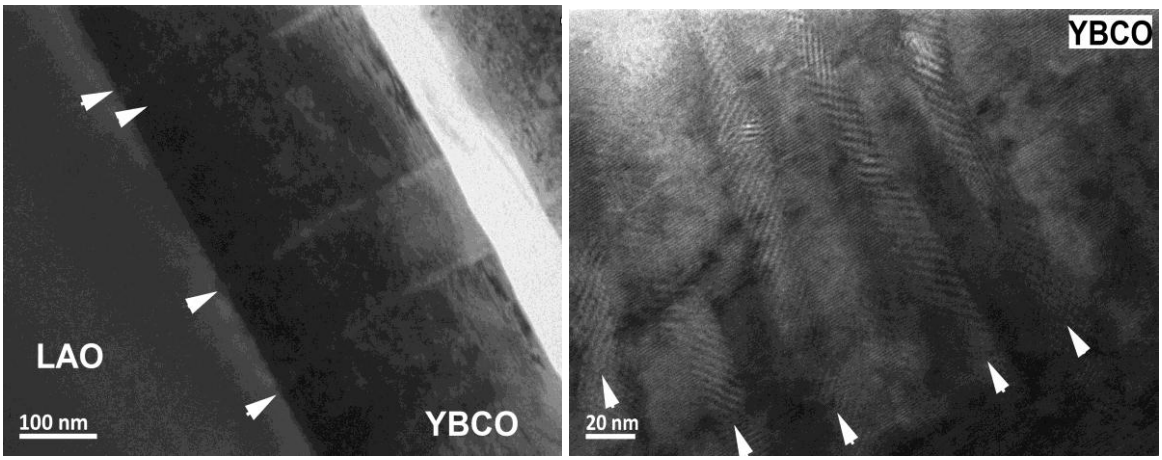

FIGURE 4. Cross-sectional TEM micrographs of YBCO+BGeO samples showing the nanocolumns at two different magnifications a) Low magnification b) High magnification

FIGURE 5 shows the x-ray diffraction patterns taken from the films indicate that the YBCO films are C- axis oriented. However reflections corresponding to BGeO of (112) orientations were noted as opposed to (002) orientations BSO peaks observed in YBCO+BSO films. The orientation relationships between BGeO and YBCO appear to be different than YBCO and BSO as the crystal structures are different. FIGURE 6 shows the cross-sectional transmission electron micrographs of YBCO+BSiO films also showing the presence of 20 nm diameter nanocolumns extending throughout the thickness of the YBCO+BSiO flms. The diameter of the nanocolumns was similar to BGeO nanocolumns observed in YBCO+BGeO.

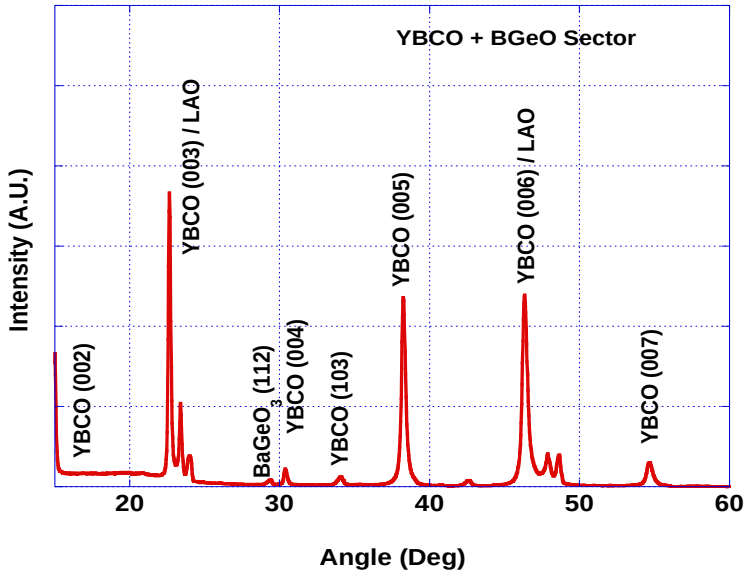

FIGURE 5. Theta- Two theta x-ray diffraction patterns of YBCO+BGeO films showing the (100) orientation of YBCO films

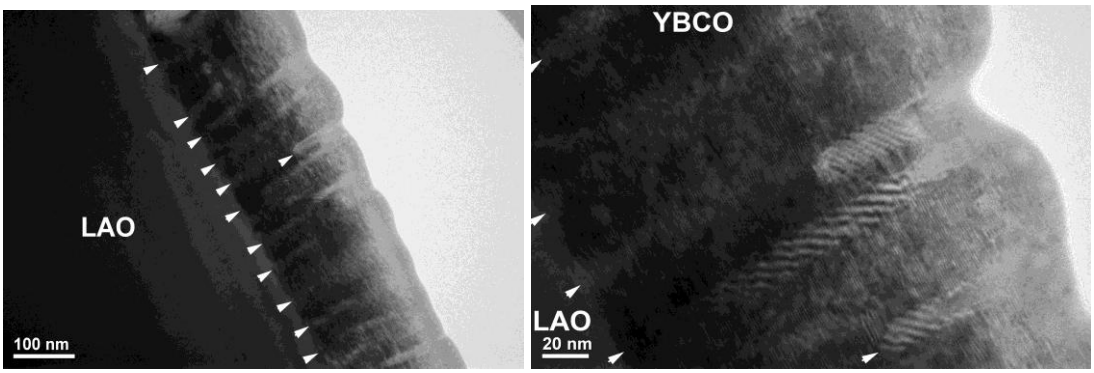

(a) (b)

FIGURE 6. Cross-sectional TEM showing the nanocolumns in YBCO+BSiO films at two different magnifications a) Low magnification b) High magnification

FIGURE 7 shows the T_c measurement of various films processed in the present study. It can be seen that the T_c is severely depressed in all the doped films. YBCO+20 mol% BGeO films had a T_c of 78 K where as YBCO+20 mol% BSO with had a T_c of 88 K. The T_c depression is thought to be due to the substitution of Ge in to YBCO lattice mostly in the Cu sites. When the doping levels are reduced from 4 mol% to 2 mol% in the case of BGeO and large sector vs. small sector in the case of BSiO, the T_c of the samples was found to improve. This trend also seems to suggest that the atomic substitutions were possibly responsible for the T_c depression. As the concentration was reduced, fewer amounts of substitutions could take place resulting in better T_c. However, the T_c is still very low even with 2 mol% BGeO giving a self field J_c of 0.7 MA/cm^2 at 77 K. The T_c was found to be reduced in YBCO+BSiO films as well and it is also thought that Si substitutions could cause the T_c drop.

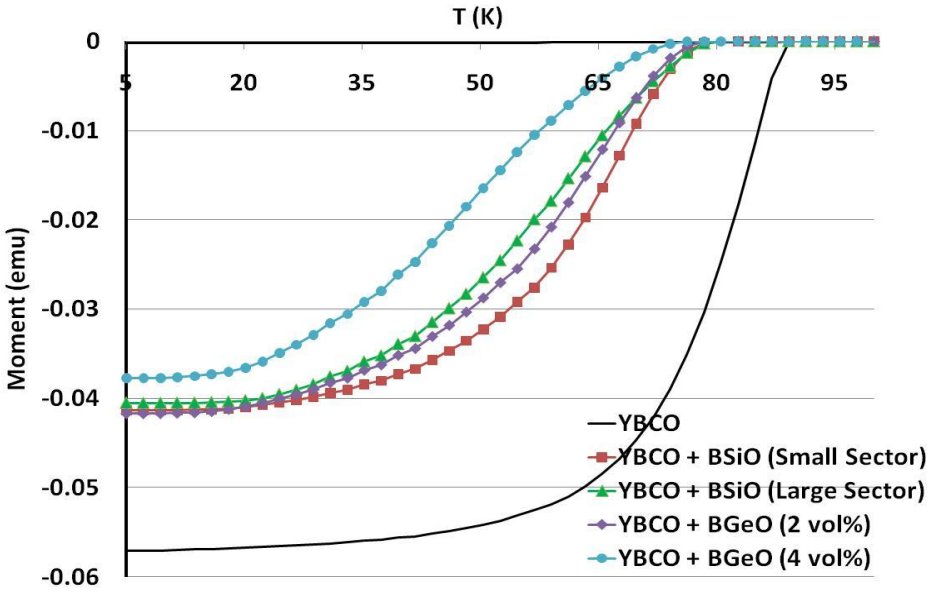

FIGURE 7. Susceptibility of YBCO+BGeO and YBCO+BSiO films showing the T_c data of different samples.

YBCO+BSO samples with BSO nanocolumns also had slightly reduced T_c of 87 K, but the T_c reduction effect on J_c was minimal. So the net effect was that J_c enhancements with the BSO nanocolumns are possible. Although the BGeO and BSiO form nanocolumns, the T_c suppression is too high to realize the advantages of having these pinning centers. It appears that the chemical compatibility of the second phases is very critical to maintain high J_c of the films. Even though the texture of YBCO was unaffected and a desired microstructure with nanocolumns was present, the T_c is reduced and the overall J_c of the films was reduced. Again, this may be due to the atomic substitutions of Ge and Si in to YBCO. While both the YBCO+BZO and YBCO+BSO systems offer a nice combination of texture maintenance, favorable T_c, and appropriate pinning centers, BSO seems to offer more flexibility in terms of the amount of additions that can be added as compared to BZO, and used as the basis for exploring this extension to additional materials more closely related to BSO.

CONCLUSIONS

High density nanocolumns of 20 nm diameter were found to form in YBCO+BGeO or YBCO+BSiO films deposited by pulsed laser ablation. The T_c of the films was found to be decreased likely due to chemical incompatibilities. As a result, the J_c of the films was reduced. With YBCO+2 vol% BGeO a self field J_c of 0.7 MA/cm^2 was observed. Both premixed and sectored targets yielded similar microstructures and film properties. Even though the nanocolumns are formed, the chemical compatibility between second phases and YBCO phases appears to be very critical to process high J_c YBCO films. This work does indicate material relationships that exist with regard to the self-assembly of second phase additions into nanocolumnar growth.

ACKNOWLEDGEMENTS

Funding Support was provided by the Air Force Office of Scientific Research (AFOSR) and the Propulsion Directorate of the Air Force Research Laboratory (AFRL). The authors would like to thank John Murphy for technical assistance.

REFERENCES

1. Larbalestier, D., Gurevich A., Feldman, D.M., and Polyanski, A., *Nature* **414**, pp 368-377 (2001).
2. Foltyn, S.R., Civale, L., Macmanus–Driscoll, J.L., Jia, Q.X., Mairov, B., Wang, H., and Maley, M., *Nat. Mater.* **6**, pp 631-642 (2007).
3. MacManus-Driscoll, J.L., Foltyn, S.R., Jia, Q.X., Wang, H., Serquis, A., Civale, L., Maiorov, B., Hawley, M.E., Maley, M.P., and Peterson, D.E., *Nat. Mater.* **3**, pp 439-443 (2004).
4. Kang, S., Goyal, A., Li, J., Gapud, A.A., Martin, P.M., Heatherly, L., Thomson, J.R., Christen, D.K., fluxList, F.A., Paranthaman, M., and Lee, D.F., *Science* **311**, pp 1911-1914 (2006)
5. Varanasi, C.V., Burke, J., Wang, H., Lee, J.H., and Barnes, P.N., *Appl. Phys. Lett.* **93**, pp 092501-092501-3 (2008)
6. Varanasi, C.V., Barnes, P.N., Burke, J., Brunke, L., Maartense, I., Haugan, T.J., Stinzianni, E.A., Dunn, K.A., Haldar, P., *Supercond. Sci. Technol*. **19** , pp L37-L41(2006)
7. Varanasi, C.V., Burke, J., Brunke, L., Wang, H., Lee, J.H., Barnes, P.N, *J. Mater. Res.* **23**, pp 3363-3369 (2008)
8. Mele, P., Matsumato, K., Ichinose, A., Mukaida, M., Yoshida, Y., Horii, S., Kita, R., *Supercond. Sci.Technol*. **21**, pp 125017-125017-6 (2008)
9. Barnes, P.N., Sumption, M.D., and Rhoads, G.L., *Cryogenics* **45**, pp 670-686 (2005).
10. Varanasi, C.V., Burke, J., Brunke, L., Wang, H., Sumption, M., Barnes, P.N., *J. Appl. Phys*. **102**, pp 063909-063909-5 (2007)
11. Guha J.P., et al., *J. of Mat. Sci*. **14**, pp 1744-1748 (1979)
12. Yamaguchi, O., Niimi, T., Shimizu, K., *Mat. Let.* **2**, pp 119-121 (1983)